Long-Lived C_{60} Radical Anion Stabilized inside an Electron-Deficient Coordination Cage

- Post-referee accepted draft -

Shota Hasegawa,[a] Shari L. Meichsner,[a] Julian J. Holstein,[a] Ananya Baksi,[a] Müge Kasanmascheff,[a] and Guido H. Clever[a*]

a. Department of Chemistry and Chem. Biology, TU Dortmund University, Otto-Hahn-Str. 6, 44227 Dortmund, Germany

KEYWORDS fullerenes, supramolecular chemistry, radicals, EPR, host-guest chemistry

ABSTRACT: Fullerene C_{60} and its derivatives are widely used in molecular electronics, photovoltaics and battery materials owing to their exceptional suitability as electron acceptors. In this context, single-electron transfer on C_{60} generates the $C_{60}^{\bullet-}$ radical anion. The short lifetime of free $C_{60}^{\bullet-}$, however, hampers its investigation and application. In this work, we dramatically stabilize the usually short-lived $C_{60}^{\bullet-}$ species within a self-assembled M_2L_4 coordination cage consisting of a triptycene-based ligand and Pd(II) cations. The electron-deficient cage strongly binds C_{60} by providing a curved inner π-surface complementarity to the fullerene's globular shape. Cyclic voltammetry revealed a positive potential shift for the first reduction of encapsulated C_{60}, indicative of a strong interaction between confined $C_{60}^{\bullet-}$ and the cationic cage. Photochemical one-electron reduction with 1-benzyl-1,4-dihydronicotinamide allows selective and quantitative conversion of the confined C_{60} molecule in millimolar acetonitrile solution at room temperature. Radical generation was confirmed by NMR, EPR, UV-Vis-NIR spectroscopy and ESI mass spectrometry. The lifetime of $C_{60}^{\bullet-}$ within the cage was found to be so large that it could still be detected after one month under inert atmosphere.

Since the discovery of fullerene C_{60} by Kroto, Smalley and Curl,[1] the football-shaped molecule has inspired scientists across a range of fields to investigate its properties, host-guest capabilities, derivatization, and application.[2-7] Nowadays, C_{60} and its derivatives have been widely applied in material science, especially in photovoltaics and organic electronics as electron-accepting and/or electron-transporting materials.[4,8-10] In organic devices, one-electron transfer from donors to C_{60} affords the $C_{60}^{\bullet-}$ radical anion. $C_{60}^{\bullet-}$ plays a key role as carrier for efficient charge harvesting.[9] Furthermore, $C_{60}^{\bullet-}$ has potential as near-infrared (NIR) dye, with possible application in bioimaging and photodynamic therapy.[11, 12] Hence, there is considerable interest to further elucidate the nature of $C_{60}^{\bullet-}$ and enhance its stability for a range of applications.[12] However, $C_{60}^{\bullet-}$ is in general a short-lived species having a lifetime lower than one second, in particular in solution at ambient conditions. Hence, *in situ* spectroscopic techniques during either bulk-electrolysis conditions or electron donation from a chemical reductant pool (such as amines) under inert conditions are required for investigating naked $C_{60}^{\bullet-}$.[13-16] Therefore, a facile method to stabilize once-generated $C_{60}^{\bullet-}$ species in solution appeared to us as a rewarding goal.

Coordination cages are three-dimensional assemblies created via metal-mediated self-assembly of organic bridging ligands with tailored shapes. Selective guest encapsulation can lead to cage-catalyzed reactions,[17-20] alter the regioselectivity of chemical transformations,[21] allow recognition of subtle structural differences between guests,[22-24] and stabilize reactive species.[25, 26]

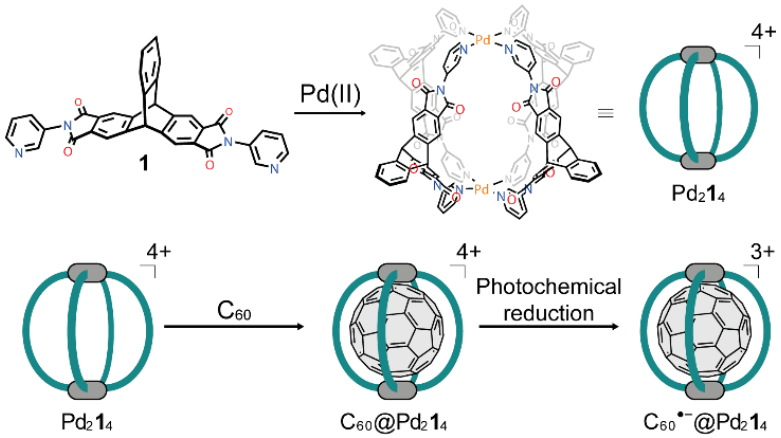

Figure 1. Structures of ligand **1** and cage $Pd_2\mathbf{1}_4$ and schematic depiction of fullerene binding and photochemical single electron reduction.

Fullerenes are attractive guest-molecules due to their globular shape and large π–surface.[27-31] A variety of fullerene complexes have been reported, with metal-mediated binders moving into focus in the last couple of years.[32-35]

Previous studies revealed that fullerene C_{60} encapsulated in cationic metallo-supramolecular assemblies shows a positive shift for the first reduction potential as compared to bulk C_{60}.[32, 33] This observation points at the prospect that the reduction product $C_{60}^{\bullet-}$ is stabilized within such coordination cages, most probably due to a combination of ionic interactions and close contacts with surrounding aromatic ligands. This hypothesis prompted us to tackle the challenge of stabilizing notoriously short-lived $C_{60}^{\bullet-}$ inside a coordination cage. We assumed that chemical reduction of already confined C_{60} is the most promising method to achieve formation of such a host-guest compound,[8, 32, 36, 37] as the lifetime of free $C_{60}^{\bullet-}$ would be much shorter than the typical encapsulation time scale, in particular when working in a heterogeneous system.[32, 33] A proper molecular design of the host is critical to allow access of a chemical reductant while shielding the formed radical anion from its surroundings to slow down dimerization or re-oxidation pathways.

Therefore, we have synthesized a lantern-shaped coordination cage $Pd_2\mathbf{1}_4$ via self-assembly of Pd(II) cations and triptycene-based bipyridyl ligand **1** featuring two phthalimide moieties.[38, 39] While the triptycene backbones offer a rather limited π–surface area for interaction with the aromatic guest, they show perfect shape-complementarity to globular C_{60}.[40, 41] Here, we show the encapsulation of C_{60} by $Pd_2\mathbf{1}_4$ and the clean generation and long-time stabilization of the $C_{60}^{\bullet-}$ radical anion inside the electron-deficient nano confinement. To the best of our knowledge, we achieved the longest lifetime of $C_{60}^{\bullet-}$ reported so far (Figure 1).

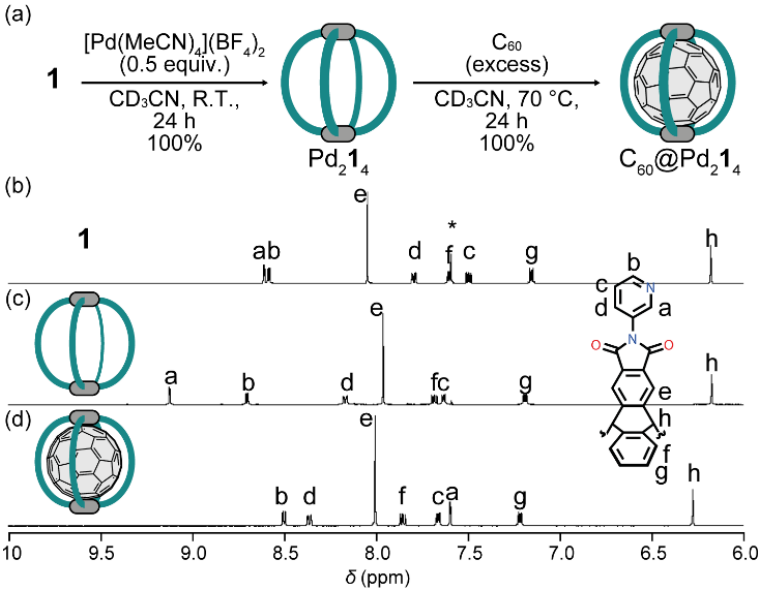

Figure 2. (a) Synthesis of $Pd_2\mathbf{1}_4$ and encapsulation of C_{60}. ^{1}H NMR spectra (CD_3CN, 500 MHz, 298 K) of (b) **1**, (c) $Pd_2\mathbf{1}_4$ and (d) $C_{60}@Pd_2\mathbf{1}_4$ (*=$CHCl_3$).

Ligand **1** was synthesized by condensation of 2,3,6,7-triptycene carboxylic dianhydride and 3-aminopyridne (Scheme S1).[42, 43] Upon heating **1** with $[Pd(CH_3CN)_4](BF_4)_2$ in acetonitrile for 24 h, $Pd_2\mathbf{1}_4$ formed quantitatively as confirmed by HR-ESI mass spectrometric and NMR spectroscopic analyses (Figure 2a). In the ^{1}H NMR spectrum, downfield-shifts were observed especially for the pyridine-donor sites due to coordination to the Pd(II) cations as previously observed for other Pd(II)-coordination cages (Figure 2b-c).[44-46]

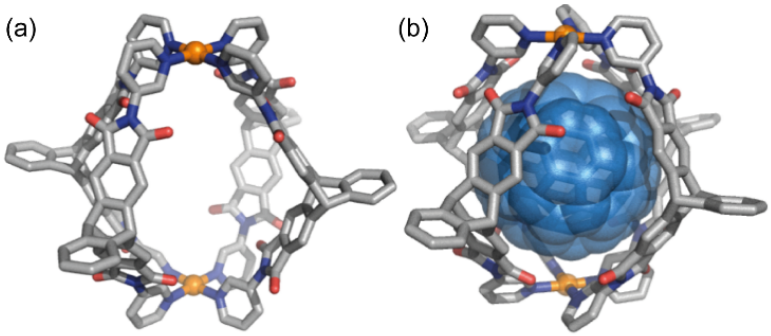

Figure 3. Single crystal X-ray structure of (a) $Pd_2\mathbf{1}_4$ and (b) $C_{60}@Pd_2\mathbf{1}_4$. Hydrogen atoms, counter anions, solvent molecules are omitted for clarity (C: gray, N: blue, O: red, Pd: orange).

Plate-like single crystals were grown by slow diffusion of diisopropylether into the acetonitrile solution of $Pd_2\mathbf{1}_4$. X-ray analysis using synchrotron radiation[47] unambiguously revealed the expected structure in the solid state (Figure 3a). VOIDOO calculations suggested about 650 Å^3 for the cavity size which is large enough to encapsulate C_{60}, occupying a volume of 547 Å^3 (Supporting

Information, Figure S19).[48] Subsequently, fullerene encapsulation into $Pd_2\mathbf{1}_4$ was carried out by dispersing an excess amount of powdered C_{60} into the acetonitrile solution of $Pd_2\mathbf{1}_4$ at 70 °C for 24 h. The transparent solution turned purple after heating, indicating C_{60} encapsulation. The formation of the host-guest complex was confirmed by ESI-MS spectrometry and NMR spectroscopy. Upon encapsulation, all ^{1}H NMR signals shifted (Figure 2d). In particular proton H^a, which is pointing inside the cavity, undergoes a significant shift, thus reflecting a drastic change of the chemical environment inside the coordination cage (Figure 2a).[38] In the ^{13}C NMR spectrum, a sharp signal was observed at 141.76 ppm belonging to encapsulated C_{60} whereas pure C_{60} is not soluble in acetonitrile. The structure of the host-guest complex was elucidated by single crystals X-ray structure analysis (Figure 3b). A slight shrinkage of the Pd•••Pd distance was observed as compared to empty $Pd_2\mathbf{1}_4$ in the solid state by 0.435(9) Å, most probably to maximize π–π interactions between the concave ligands and convex C_{60} (Figure S14-15).

The electron deficient character of **1**, combined with its coordination to the cationic metal nodes, prompted us to investigate the electronic properties of the C_{60} molecule inside the coordination cage. Usually, bulk C_{60} shows a first reduction wave around –1.0 V in organic solvents versus the first oxidation potential of ferrocene.[49] Cyclic voltammetry applied to empty cage $Pd_2\mathbf{1}_4$ revealed a first reduction wave at –1.78 V, assignable to a reduction of the ligand (Figure 4a). On the other hand, the cyclic voltammogram of $C_{60}@Pd_2\mathbf{1}_4$ showed several irreversible reduction waves at less negative potentials besides the reversible cage reduction at –1.79 V (Figure 4b). The newly observed signals can be attributed to stepwise reduction steps of the confined C_{60} molecule. This result was also supported by DFT calculations implying that the LUMO should be localized on the C_{60} molecule within the host-guest complex (Figure 4d). The first reduction potential for the encapsulated C_{60} molecule was observed at –0.48 V as a reversible wave when the measurement was run within a narrower window from –0.7 V to –0.2 V (vs. Fc/Fc^+; Figure 4c). Noteworthy, this value is the least negative potential value for C_{60} molecules encapsulated in coordination cages reported so far.[32, 33] This result suggests significant interaction between the reduced anionic species $C_{60}^{\bullet-}$ and the cationic cage (Table S3). Gas-phase DFT calculations indeed indicate that $C_{60}^{\bullet-}$ should be much stronger bound than C_{60} (Supporting Information).

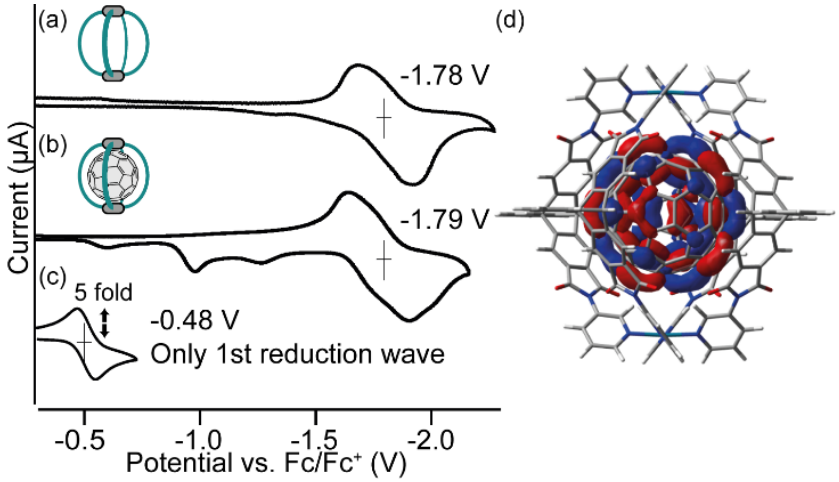

Figure 4. Cyclic voltammograms (0.1 M $TBAPF_6$, 100 mV/s, 0.70 mM, acetonitrile) of (a) $Pd_2\mathbf{1}_4$, (b) $C_{60}@Pd_2\mathbf{1}_4$ and (c) $C_{60}@Pd_2\mathbf{1}_4$ measured within a potential window from –0.7 V to –0.2 V (vs. Fc/Fc^+). (d) LUMO of $C_{60}@Pd_2\mathbf{1}_4$ calculated with M06-2X DFT functional and Lanl2dz basis set for Pd atoms and 6-31G(d,p) for other atoms with PCM solvent consideration (geometry optimized on M06-2X/Lanl2dz level).

Next, we explored the chemical reduction and stabilization of formed $C_{60}^{\bullet-}$ in the cage. 1-Benzyl-1,4-dihydronicotinamide (BNAH) is the most suitable photochemical one-electron reductant as described by Fukuzumi.[50] In the reduction process, C_{60} itself works as a photosensitizer to activate BNAH by an energy transfer from its excited triplet state. ^{1}H NMR showed that $C_{60}@Pd_2\mathbf{1}_4$ is stable in the presence of 0.5 equivalent of BNAH in the dark (Figure 5d). The mixture was irradiated with a white LED light source for 2 mins and a ^{1}H NMR spectrum was measured immediately after irradiation (Figure 5a). Interestingly, all ^{1}H NMR signals of $C_{60}@Pd_2\mathbf{1}_4$ broadened while BNAH was completely transformed into the corresponding oxidized species (Figure 5c). It is known that ^{1}H NMR signals broaden when host-molecules are accommodating radical species due to accelerated nuclear spin relaxation processes.[51, 52] Subsequently, the broadened signals became again sharper over time due to deactivation of the radical species. Surprisingly, the decay of the radical species lasted for at least 2 h despite the aerobic atmosphere the acetonitrile solution was exposed to (Figures 5b, S23). It should be noted that photochemical reduction did not take place with only $Pd_2\mathbf{1}_4$ (Figure S24). In addition, only $C_{60}@Pd_2\mathbf{1}_4$ but not empty $Pd_2\mathbf{1}_4$ gave broadened signals when a 1:1 mixture of $C_{60}@Pd_2\mathbf{1}_4$ and $Pd_2\mathbf{1}_4$ was irradiated in the presence of BNAH (Figure S25). These control experiments suggested that not the cage but the confined C_{60} is reduced. Furthermore, we measured ESI-MS right after photochemical reduction. As a result, a prominent signal corresponding to a one-electron-reduced $[C_{60}@Pd_2\mathbf{1}_4]^{3+}$ species was observed (Figure 5e). These results further supported formation of $C_{60}^{\bullet-}$ and its stabilization inside $Pd_2\mathbf{1}_4$.

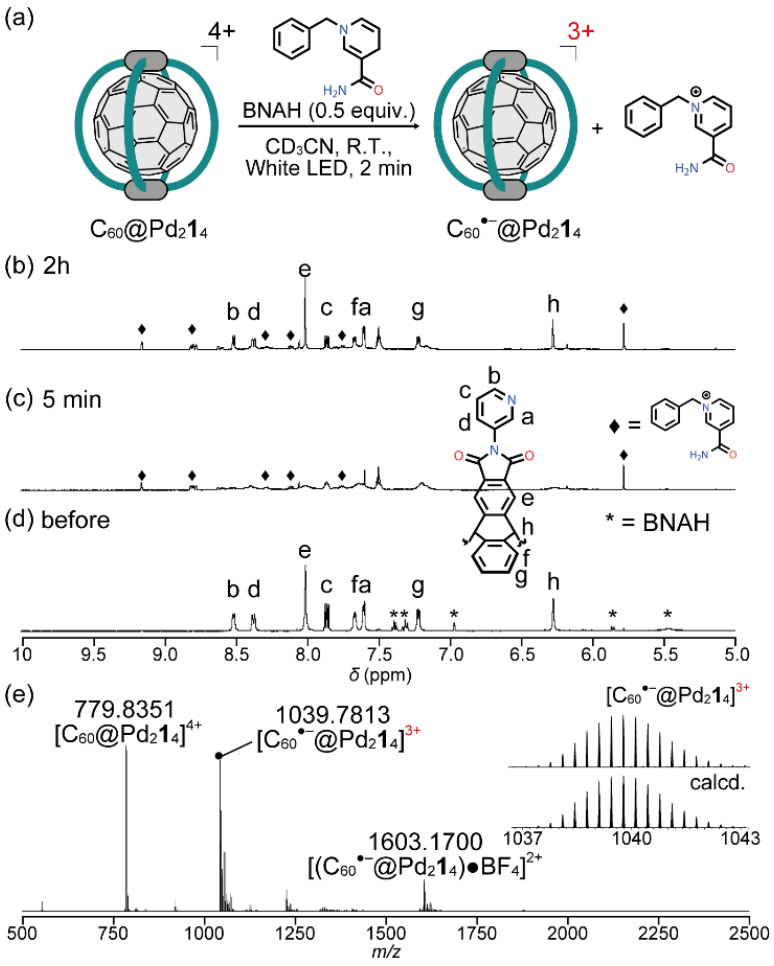

Figure 5. (a) Photochemical reduction of C_{60}@Pd_2**1**$_4$. ^{1}H NMR spectra measured after (b) 2 h, (c) 5 mins and (d) before irradiation. (e) ESI-MS spectrum of $C_{60}^{\bullet-}$@Pd_2**1**$_4$.

$C_{60}^{\bullet-}$ is known to show a characteristic absorption in the NIR region.[13-15] A UV-Vis-NIR spectrum was measured immediately after photochemical reduction. As a result, new absorption bands at 975 and 1111 nm were observed while the encapsulated C_{60} showed absorption at 546 and 599 nm before reduction (Figure 6a). The observed spectral characteristics are in very good accordance with $C_{60}^{\bullet-}$ absorption spectra reported in the past.[13-15, 37] The absorption intensity decreased over time due to re-oxidation of encapsulated $C_{60}^{\bullet-}$. The half-lifetime of $C_{60}^{\bullet-}$ was estimated to be 13 mins by following the decline of the 1111 nm absorption in aerated acetonitrile solution at 298 K (Figure S27). The observed NIR absorptions showed a red-shift by about 20-30 nm compared with the reported absorption of naked $C_{60}^{\bullet-}$. It is known that both absorptions originate from an electron transition from SOMO to LUMO levels.[13] According to resonance Raman spectroscopy studies, two totally symmetric A_g vibrational modes are the reason for the observed splitting.[13,53] Therefore, modulation of the molecular vibrations within $C_{60}^{\bullet-}$ is suspected as reason for the red-shift observed in the absorption spectrum, most probably due to the close confinement of the radical anion within the inner space of cationic host Pd_2**1**$_4$. We further could show that the encapsulated $C_{60}^{\bullet-}$ radical anion can be rapidly and cleanly re-oxidized by adding tetracyanoethylene (TCNE) as confirmed by NMR and MS analyses (Figure S39, S40).

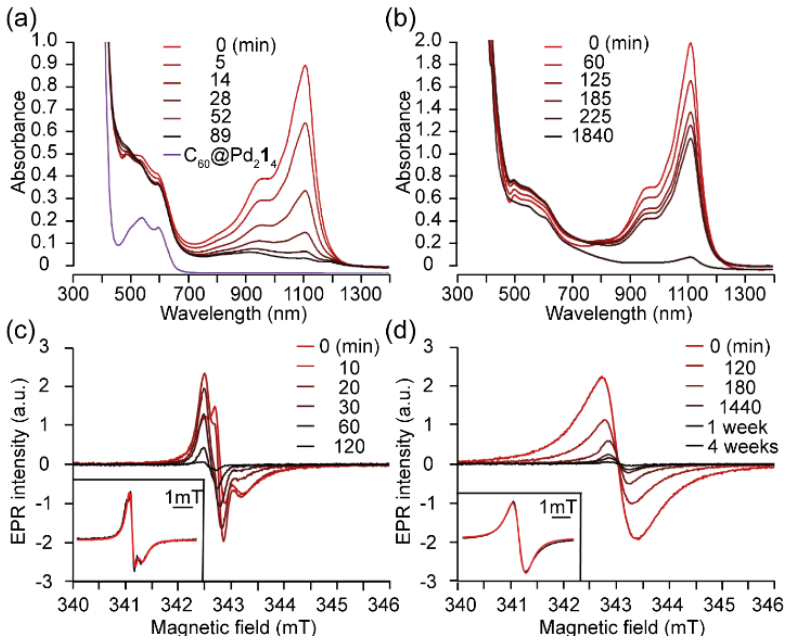

Figure 6. UV-Vis-NIR spectra (acetonitrile, 0.35 mM, 298 K) of $C_{60}^{\bullet-}$@Pd_2**1**$_4$ measured in (a) aerobic conditions and (b) under N_2 atmosphere over time. Time-dependent EPR spectra of $C_{60}^{\bullet-}$@Pd_2**1**$_4$ prepared under (c) aerobic conditions and (d) in N_2 atmosphere, both recorded at X-band and at 100 K. The corresponding simulations of the EPR spectra (red) are shown in the inset (for details see SI).

We further investigated the lifetime of $C_{60}^{\bullet-}$ inside Pd_2**1**$_4$ in inert atmosphere (Figure 6b). Identical absorptions were observed in the NIR region but their decline was significantly lengthened by removing oxygen. Subsequently, X-band EPR spectra were measured for the samples prepared in air and inert atmosphere at 100 K. The $C_{60}^{\bullet-}$ signal, having an isotropic *g* value of 1.999, was detected in both samples (Figure 6c and d, see S36 for details). In case of the sample prepared in air, an additional signal with g_{iso} = 2.001 arising from an oxygenated species was observed (Figure 6c).[54] The existence of such oxygenated species was also confirmed unambiguously by ESI-MS analysis (Figure S32, S33). In contrast, encapsulated $C_{60}^{\bullet-}$ was the only paramagnetic species observed in the sample prepared under N_2 atmosphere (Figure 6d). The half-lifetime of $C_{60}^{\bullet-}$ was estimated to be 14 min under aerobic conditions, in full agreement with the value obtained by UV-Vis-NIR spectroscopy. Under inert atmosphere conditions, aliquot-based EPR measurements delivered a half-lifetime of 893 min while direct monitoring of the radical decay by UV-Vis-NIR spectroscopy at room temperature pointed to a half-lifetime of about 300 min (see SI for discussion of possible reasons of this deviation). Astonishingly, the EPR signal of the encapsulated $C_{60}^{\bullet-}$ could be still observed after one month (within the EPR instrument's detection limit in the low micromolar range), which – to the best of our knowledge – is the longest lifetime reported for the $C_{60}^{\bullet-}$ radical anion so far (Figure S38).

In conclusion, we deliver the encapsulation and long-time stabilization of photochemically generated $C_{60}^{\bullet-}$ inside a lantern-shaped coordination cage. The electron deficient cage tightly binds the anionic guest and serves as a protecting group to shield the radical species, most probably by kinetically hampering access of oxidants. We believe that our system represents an important step towards application of $C_{60}^{\bullet-}$ for various chemical, spectroscopic and imaging purposes. This well-behaved spin-system should further be attractive for EPR labelling chemistry, molecular magnetism and material science applications.

ASSOCIATED CONTENT

Supporting Information

Synthetic procedures, NMR, MS, UV-Vis-NIR, EPR, crystallographic analysis, and DFT calculations. The Supporting Information is available free of charge on the ACS Publications website.

AUTHOR INFORMATION

Corresponding Author

* Guido, H. Clever, guido.clever@tu-dortmund.de

ACKNOWLEDGMENT

S.H. thanks the DAAD for a PhD fellowship. This work was funded by the Deutsche Forschungsgemeinschaft (DFG, German Research Foundation) under Germany's Excellence Strategy – EXC 2033 – 390677874 – RESOLV and GRK2376 "Confinement-controlled Chemistry" -

project number 331085229. Diffraction data of Pd_2**1**$_4$ and C_{60}@Pd_2**1**$_4$ was collected at PETRA III, DESY at synchrotron beamline P11 (I-20191452, I-20200144). S.H. and G.H.C. thank Prof. Andreas Steffen and Dr. Benjamin Hupp for access to the UV-Vis-NIR spectrometer and Dr. Jacopo Tessarolo for help with the kinetic analyses.

This work is dedicated to the memory of François Diederich.

REFERENCES

(1) Kroto, H. W.; Heath, J. R.; O'Brien, S. C.; Curl, R. F.; Smalley, R. E. C_{60}: Buckminsterfullerene. *Nature* **1985**, *318* (6042), 162–163.
(2) Balch, L. A.; Olmstead, M. M. Reactions of Transition Metal Complexes with Fullerenes (C60, C70, etc.) and Related Materials. *Chem. Rev.* **1998**, *98*, 2123–2165.
(3) Sawamura, M.; Kawai, K; Matsuo, Y.; Kanie, K.; Kato, T.; Nakamura, E. Stacking of conical molecules with a fullerene apex into polar columns in crystals and liquid crystals. *Nature* **2002**, *419*, 702–705.
(4) Dennler, G.; Scharber, C. M.; Brabec, J. C. Polymer-Fullerene Bulk-Heterojunction Solar Cells. *Adv. Mater.* **2009**, *21*, 1323–1338.
(5) Maeda-Mamiya, R.; Noiri, E.; Isobe, H.; Nakanishi, W.; Okamoto, K.; Doi, K.; Sugaya, T.; Izumi, T.; Homma, T.; Nakamura, E. In Vivo Gene Delivery by Cationic Tetraamino Fullerene. *Proc. National. Acad. Sci.* **2010**, *107* (12), 5339–5344.
(6) Winkelmann, C. B.; Roch, N.; Wernsdorfer, W.; Bouchiat, V.; Balestro, F. Superconductivity in a Single C_{60} Transistor. *Nat. Phys.* **2009**, *5* (12), 876–879.
(7) Leung, F. K.-C.; Ishiwari, F.; Kajitani, T.; Shoji, Y.; Hikima, T.; Takata, M.; Saeki, A.; Seki, S.; Yamada, Y. M. A.; Fukushima, T. Supramolecular Scaffold for Tailoring the Two-Dimensional Assembly of Functional Molecular Units into Organic Thin Films. *J. Am. Chem. Soc.* **2016**, *138* (36), 11727–11733.
(8) Guldi, D. M.; Prato, M. Excited-State Properties of C60 Fullerene Derivatives. *Acc. Chem. Res.* **2000**, *33* (10), 695–703.
(9) Pivrikas, A.; Sariciftci, N. S.; Juška, G.; Österbacka, R. A Review of Charge Transport and Recombination in Polymer/Fullerene Organic Solar Cells. *Prog. Photovoltaics. Res. Appl.* **2007**, *15* (8), 677–696.
(10) Umeyama, T.; Imahori, H. Isomer Effects of Fullerene Derivatives on Organic Photovoltaics and Perovskite Solar Cells. *Acc. Chem. Res.* **2019**, *52* (8), 2046–2055.
(11) Fabian, J.; Nakazumi, H.; Matsuoka, M. Near Infrared Absorbing Dyes: *Chem. Rev.* **1998**, *92*, 1197–1226.
(12) Pansare, V. J.; Hejazi, S.; Faenza, W. J.; Prud'homme, R. K. Review of Long-Wavelength Optical and NIR Imaging Materials: Contrast Agents, Fluorophores, and Multifunctional Nano Carriers. *Chem. Mater.* **2012**, *24* (5), 812–827.
(13) Kato, T.; Kodama, T.; Shida, T.; Nakagawa, T.; Matsui, Y.; Suzuki, S.; Shiromaru, H.; Yamauchi, K.; Achiba, Y. Electronic Absorption Spectra of the Radical Anions and Cations of Fullerenes: C_{60} and C_{70}. *Chem. Phys. Lett.* **1991**, *180* (5), 446–450.
(14) Gasyna, Z.; Andrews, L.; Schatz, P. N. Near-Infrared Absorption Spectra of Fullerene (C_{60}) Radical Cations and Anions Prepared Simultaneously in Solid Argon. *J. Phys. Chem.* **1992**, *96* (4), 1525–1527.
(15) Lobach, A. S.; Goldshleger, N. F.; Kaplunov, M. G.; Kulikov, A. V. Near-IR and ESR Studies of the Radical Anions of C_{60} and C_{70} in the System Fullerene-Primary Amine. *Chem. Phys. Lett.* **1995**, *243* (1–2), 22–28.
(16) Friedrich, J.; Schweitzer, P.; Dinse, K.-P.; Rapta, P.; Stasko, A. EPR Study of Radical Anions of C_{60} and C_{70}. *Appl. Magn. Reson.* **1994**, *7* (2–3), 415–425.
(17) Yoshizawa, M.; Miyagi, S.; Kawano, M.; Ishiguro, K.; Fujita, M. Alkane Oxidation via Photochemical Excitation of a Self-Assembled Molecular Cage. *J. Am. Chem. Soc*. **2004**, *126* (30), 9172–9173.
(18) Kusukawa, T.; Nakai, T.; Okano, T.; Fujita, M. Remarkable Acceleration of Diels–Alder Reactions in a Self-Assembled Coordination Cage. *Chem. Lett.* **2003**, *32* (3), 284–285.
(19) Young, T. A.; Martí-Centelles, V.; Wang, J.; Lusby, P. J.; Duarte, F. Rationalizing the Activity of an "Artificial Diels-Alderase": Establishing Efficient and Accurate Protocols for Calculating Supramolecular Catalysis. *J. Am. Chem. Soc.* **2019**, *142* (3), 1300–1310.
(20) Spicer, R. L.; Stergiou, A. D.; Young, T. A.; Duarte, F.; Symes, M. D.; Lusby, P. J. Host–Guest-Induced Electron Transfer Triggers Radical-Cation Catalysis. *J. Am. Chem. Soc.* **2020**, *142*, 5, 2134-2139.
(21) Yoshizawa, M.; Tamura, M.; Fujita, M. Diels-Alder in Aqueous Molecular Hosts: Unusual Regioselectivity and Efficient Catalysis. *Science* **2006**, *312* (5771), 251–254.
(22) Yamashina, M.; Akita, M.; Hasegawa, T.; Hayashi, S.; Yoshizawa, M. A Polyaromatic Nanocapsule as a Sucrose Receptor in Water. *Sci. Adv.* **2017**, *3* (8), e1701126.
(23) Yamashina, M.; Kusaba, S.; Akita, M.; Kikuchi, T.; Yoshizawa, M. Cramming versus Threading of Long Amphiphilic Oligomers into a Polyaromatic Capsule. *Nat. Commun.* **2018**, *9* (1), 4227.
(24) Yamashina, M.; Tsutsui, T.; Sei, Y.; Akita, M.; Yoshizawa, M. A Polyaromatic Receptor with High Androgen Affinity. *Sci. Adv.* **2019**, *5* (4), eaav3179.
(25) Mal, P.; Breiner, B.; Rissanen, K.; Nitschke, J. R. White Phosphorus Is Air-Stable Within a Self-Assembled Tetrahedral Capsule. *Science* **2009**, *324* (5935), 1697–1699.
(26) Yamashina, M.; Sei, Y.; Akita, M.; Yoshizawa, M. Safe Storage of Radical Initiators within a Polyaromatic Nanocapsule. *Nat Commun* **2014**, *5* (1), 4662.
(27) Kawase, T.; Kurata, H. Ball-, Bowl-, and Belt-Shaped Conjugated Systems and Their Complexing Abilities: Exploration of the Concave−Convex π−π Interaction. *Chem. Rev.* **2006**, *106* (12), 5250–5273.
(28) García-Simón, C.; Costas, M.; Ribas, X. Metallosupramolecular Receptors for Fullerene Binding and Release. *Chem. Soc. Rev.* **2015**, *45* (1), 40–62.
(29) Sun, D.; Tham, F. S.; Reed, C. A.; Chaker, L.; Burgess, M.; Boyd, P. D. W. Porphyrin−Fullerene Host−Guest Chemistry. *J. Am. Chem. Soc.* **2000**, *122* (43), 10704–10705.
(30) Iwamoto, T.; Watanabe, Y.; Sadahiro, T.; Haino, T.; Yamago, S. Size-Selective Encapsulation of C_{60} by [10]Cycloparaphenylene: Formation of the Shortest Fullerene-Peapod. *Angew. Chem., Int. Ed.* **2011**, *50* (36), 8342–8344.
(31) Selmani, S.; Schipper, D. J. π-Concave Hosts for Curved Carbon Nanomaterials. *Chem. Eur. J.* **2019**, *25* (27), 6673–6692.

(32) Rizzuto, F. J.; Wood, D. M.; Ronson, T. K.; Nitschke, J. R. Tuning the Redox Properties of Fullerene Clusters within a Metal-Organic Capsule. *J. Am. Chem. Soc.* **2017**, *139* (32), 11008–11011.
(33) Matsumoto, K.; Kusaba, S.; Tanaka, Y.; Sei, Y.; Akita, M.; Aritani, K.; Haga, M.; Yoshizawa, M. A Peanut-Shaped Polyaromatic Capsule: Solvent-Dependent Transformation and Electronic Properties of a Non-Contacted Fullerene Dimer. *Angew. Chem., Int. Ed.* **2019**, *58* (25), 8463–8467.
(34) Yu, X.; Wang, B.; Kim, Y.; Park, J.; Ghosh, S.; Dhara, B.; Mukhopadhyay, R. D.; Koo, J.; Kim, I.; Kim, S.; Hwang, I.-C.; Seki, S.; Guldi, D. M.; Baik, M.-H.; Kim, K. Supramolecular Fullerene Tetramers Concocted with Porphyrin Boxes Enable Efficient Charge Separation and Delocalization. *J. Am. Chem. Soc*. **2020**, *142* (29), 12596–12601.
(35) Barendt, T. A.; Myers, W. K.; Cornes, S. P.; Lebedeva, M. A.; Porfyrakis, K.; Marques, I.; Félix, V.; Beer, P. D. The Green Box: An Electronically Versatile Perylene Diimide Macrocyclic Host for Fullerenes. *J. Am. Chem. Soc.* **2019**, 1*42*, 349–364.
(36) Imahori, H.; Mori, Y.; Matano, Y. Nanostructured Artificial Photosynthesis. *J. Photochem. Photobiology. C. Photochem. Rev.* **2003**, *4* (1), 51–83.
(37) Kato, T.; Kodama, T.; Oyama, M.; Okazaki, S.; Shida, T.; Nakagawa, T.; Matsui, Y.; Suzuki, S.; Shiromaru, H.; Yamauchi, K.; Achiba, Y. ESR and Optical Studies of the Radical Anion of C_{60}. *Chem. Phys. Lett.* **1991**, *186* (1), 35–39.
(38) Chen, B.; Holstein, J. J.; Horiuchi, S.; Hiller, W. G.; Clever, G. H. Pd(II) Coordination Sphere Engineering: Pyridine Cages, Quinoline Bowls, and Heteroleptic Pills Binding One or Two Fullerenes. *J. Am. Chem. Soc.* **2019**, *1414*, 8907–8913.
(39) Chen, B.; Horiuchi, S.; Holstein, J. J.; Tessarolo, J.; Clever, G. H. Tunable Fullerene Affinity of Cages, Bowls and Rings Assembled by Pd(II) Coordination Sphere Engineering. *Chem. Eur. J.* **2019**, *25*, 14921–14927.
(40) Veen, E. M.; Feringa, B. L.; Postma, P. M.; Jonkman, H. T.; Spek, A. L. Solid State Organisation of C_{60} by Inclusion Crystallisation with Triptycenes. Chem. Commun. **1999**, *0* (17), 1709–1710.
(41) Mondal, S.; Chakraborty, S.; Bhowmick, S.; Das, N. Synthesis of Triptycene-Based Organosoluble, Thermally Stable, and Fluorescent Polymers: Efficient Host–Guest Complexation with Fullerene. *Macromolecules* **2013**, *46*, 6824–6831.
(42) Xiao, Y.-H.; Shao, Y.; Ye, X.-X.; Cui, H.; Wang, D.-L.; Zhou, X.-H.; Sun, S.-L.; Cheng, L. Microporous Aromatic Polyimides Derived from Triptycene-Based Dianhydride. *Chin*. *Chem*. *Lett*. **2016**, *27* (3), 454–458.
(43) Clever, G. H.; Tashiro, S.; Shionoya, M. Inclusion of Anionic Guests inside a Molecular Cage with Palladium(II) Centers as Electrostatic Anchors. *Angew. Chem., Int. Ed.* **2009**, *48* (38), 7010–7012.
(44) Clever, G. H.; Punt, P. Cation–Anion Arrangement Patterns in Self-Assembled Pd_2L_4 and Pd_4L_8 Coordination Cages. *Acc. Chem. Res.* **2017**, *50* (9), 2233–2243.
(45) Han, M.; Engelhard, D. M.; Clever, G. H. Self-Assembled Coordination Cages Based on Banana-Shaped Ligands. *Chem. Soc. Rev.* **2014**, *43* (6), 1848–1860.
(46) Saha, S.; Regeni, I.; Clever, G. H. Structure Relationships between Bis-Monodentate Ligands and Coordination Driven Self-Assemblies. *Coord. Chem. Rev*. **2018**, *374*, 1–14.
(47) A. Burkhardt, T. Pakendorf, B. Reime, J. Meyer, P. Fischer, N. Stübe, S. Panneerselvam, O. Lorbeer, K. Stachnik, M. Warmer, P. Rödig, D. Göries and A. Meents, *Eur. Phys. J. Plus* **2016**, *131*, 56.
(48) Adams, G. B.; O'Keeffe, M.; Ruoff, R. S. Van Der Waals surface areas and volumes of fullerenes. *J. Phys. Chem.* **1994**, *98*, 9465−9469.
(49) Allemand, P. M.; Koch, A.; Wudl, F.; Rubin, Y.; Diederich, F.; Alvarez, M. M.; Anz, S. J.; Whetten, R. L. Two Different Fullerenes Have the Same Cyclic Voltammetry. *J. Am. Chem. Soc.* **1991**, *113* (3), 1050–1051.
(50) Fukuzumi, S.; Suenobu, T.; Patz, M.; Hirasaka, T.; Itoh, S.; Fujitsuka, M.; Ito, O. Selective One-Electron and Two-Electron Reduction of C_{60} with NADH and NAD Dimer Analogues via Photoinduced Electron Transfer. *J. Am. Chem. Soc.* **1998**, *120* (32), 8060–8068.
(51) Futagoishi, T.; Aharen, T.; Kato, T.; Kato, A.; Ihara, T.; Tada, T.; Murata, M.; Wakamiya, A.; Kageyama, H.; Kanemitsu, Y.; Murata, Y. A Stable, Soluble, and Crystalline Supramolecular System with a Triplet Ground State. *Angew. Chem., Int. Ed.* **2017**, *56* (15), 4261–4265.
(52) Hasegawa, S.; Hashikawa, Y.; Kato, T.; Murata, Y. Construction of a Metal-Free Electron Spin System by Encapsulation of an NO Molecule Inside an Open-Cage Fullerene C_{60} Derivative. *Angew. Chem., Int. Ed.* **2018**, *57* (39), 12804–12808.
(53) Bethune, D. S.; Meijer, G.; Tang, W. C.; Rosen, H. J. The Vibrational Raman Spectra of Purified Solid Films of C_{60} and C_{70}. *Chem. Phys. Lett.* **1990**, *174* (3–4), 219–222.
(54) Paul, P.; Kim, K. -C.; Sun, D.; Boyd, D. W. P.; Reed, A. C. Artifacts in the Electron Paramagnetic Resonance Spectra of C_{60} Fullerene Ions: Inevitable $C_{120}O$ Impurity. *J. Am. Chem. Soc.* **2002**, *124* (16), 4394–4401.